applied sciences

MDPI

Article

Experimental Study on Radiation Noise Frequency Characteristics of a Centrifugal Pump with Various Rotational Speeds

Chang Guo [1], Ming Gao [1,*], Dongyue Lu [2] and Hongjun Guan [3]

1 School of Energy and Power Engineering, Shandong University, Jinan 250061, China; gg3263@163.com
2 State Nuclear Power Engineering Company, Shanghai 200233, China; ldy11energy@163.com
3 Shengli Power Plant, Dongying 257087, China; guanhongjun999.slyt@sinopec.com
* Correspondence: gm@sdu.edu.cn; Tel.: +86-531-8839-9008

Received: 12 April 2018; Accepted: 13 May 2018; Published: 16 May 2018

Abstract: To investigate the radiation noise frequency characteristics of a centrifugal pump under various rotational speeds, a noise measurement system was established in a soundproof room. Sixteen monitoring points were evenly arranged in a circumferential direction around the pump and the sound pressure levels (SPLs) at different monitoring points were measured by a microphone, then the changing patterns of radiation noise in a wide frequency range and at certain frequencies were studied. The results reveal that the SPLs reach a maximum between 1000 and 2000 Hz, while SPLs are lower in other frequency ranges. Additionally, the acoustic energy was introduced to determine the proportion of radiation noise in different frequency ranges to overall noise. When rotational speed increases from 1700 to 2900 rpm, the proportion of acoustic energy between 1000 and 2000 Hz is higher than 0.50 and shows an increasing trend. Meanwhile, the proportion between 0 and 1000 Hz is about 0.30 and decreases gradually, while that between 2000 and 8000 Hz is about 0.12 and shows little change. Also, the increase in radiation noise at high frequency is higher than that at low frequency. This study could provide theoretical guidance for research regarding radiation noise prediction and control technology at different frequencies of centrifugal pumps.

Keywords: frequency characteristics; radiation noise; acoustic energy; centrifugal pump; experimental study

1. Introduction

The problem of noise has drawn widespread attention and has been the subject of studies in recent years [1–3]. Centrifugal pumps are extensively applied in many fields related to the national economy [4,5]. During the operation of pumps, due to the periodic rotation of rotating parts, the flow inside the pumps and the interference between impeller and volute are both repetitive, and cause periodic pressure fluctuations in the flow field, consequently, repetitive impulsive noise [6] is generated. The noise generated by centrifugal pumps can affect human health, degrade the pump flow performance, consume extra external energy and depreciate the working environment [7]. As the regulations for environmental noise become increasingly strict, methods that lower the noise are becoming more significant. Therefore, it is crucial to have a better understanding of radiation noise frequency characteristics, to provide theoretical guidance for research on radiation noise prediction and control technology at different frequencies of centrifugal pumps.

In the past, considerable research has been carried out in terms of the frequency characteristics of centrifugal pump noise. Rzentkowski and Zbroja [8,9] experimentally analyzed the dynamic pressure pulsations spectrum at the pump discharge site, and summarized that the blade-passing excitation

amplitude is the highest amplitude in the pressure spectrum. Parrondo et al. [10] analyzed the inner sound field in low frequency ranges and reported that the inner sound field could be characterized by a dipole-like source located near the tongue. Si et al. [11] found that the blade-passing frequency (BPF) and its harmonic frequencies are the main frequencies of the flow noise in pipelines and the sound pressure level (SPL) at BPF is higher than the others. Yang et al. [12] reported that the SPL at BPF reached a peak value near the volute tongue. As is known, centrifugal pumps always work in various conditions with various working demands, Ke [13] concluded that the change of flow rate had a great influence on flow noise, especially on the SPL at BPF. Using the near field acoustic pressure method, Ye et al. [14] measured radiation noise under various flow rate conditions, and discovered that the SPLs with a high frequency of 1000 and 2000 Hz made a significant contribution to the overall A-weighted sound pressure level.

With the development of computational fluid dynamics (CFD) technology, numerical calculation methods have been widely adopted by scholars [15,16]. A hybrid method combining CFD with Lighthill acoustic analogy has been widely used to elucidate and predict acoustic generation [17–19]. Langthjem et al. [20,21] applied it for noise calculation in a two-dimensional centrifugal pump and concluded that the main noise source was the dipole source. The dipole source was defined as an unsteady fluid force acting on the wall surface, including the impeller dipole source and the volute dipole source in centrifugal pumps. The impeller-generated radiation noise at BPF exhibited obvious dipole characteristic behavior [22], while the volute-generated radiation noise clearly showed asymmetric directivity characteristics, i.e., the radiation noise in the direction facing the tongue was higher than that in the direction against the tongue [23]. Liu et al. [24] also validated the important impact of the pump cavity dipole source on calculation results. In addition, the pump structure modal response was considered to obtain more accurate results, Ding et al. [25] studied the effect of different structures on SPL at BPF and provided guidance for structural optimization of centrifugal pumps.

Obviously, radiation noise has direct impacts on living and working environments. According to the above literature review, previous experimental research has mainly focused on the internal flow noise characteristics in centrifugal pump pipes, while little experimental research has focused on radiation noise outside the pumps. Additionally, the SPLs at each order of BPF have been the main concern of both experimental and numerical studies. However, it seems clear that the noise radiated by centrifugal pumps is a kind of broadband noise and it has different characteristics at different frequencies, thus, it is necessary to find out the radiation noise distribution in a wide frequency range. In general, pumps work in various conditions with various working demands and the radiation noise at different frequencies changes accordingly, so it is also necessary to study various operational conditions for radiation noise.

Therefore, a centrifugal pump radiation noise measurement system was established in a soundproof room. Then, the changing patterns of radiation noise in a wide frequency range and the proportion of noise in different frequency ranges to overall noise, as well as the noise at certain frequencies were analyzed under various rotational speeds. The conclusions could lay the foundation for further research regarding radiation noise prediction and control technology at different frequencies of centrifugal pumps.

2. Experimental Facility and Procedure

2.1. Parameters of the Test Pump

The test is conducted with a single-stage pump, water at normal temperature is used as working fluid. The geometric and performance parameters of the test pump are listed in Table 1.

Table 1. Geometric and performance parameters of the test pump.

Parameter	Value
Inlet diameter, mm	80
Impeller diameter, mm	250
Outlet diameter, mm	50
Rated flow rate, m^3/h	50
Design head, m	80
Rated rotational speed, rpm	2900
Blade number	6
Blade-passing frequency, Hz	290
Shaft-passing frequency, Hz	48.3

2.2. Radiation Noise Measurement System

As shown in Figure 1, the experimental apparatuses include a soundproof room, water circulation system, circuit control system, data acquisition and storage system. During the operation, to absorb the external noise and reduce the influence of the surrounding environment and motor operation on the measurement results, the motor and centrifugal pump were insulated in a soundproof room; the exterior walls of the soundproof room, along with the motor, were clad with soundproof cotton. In addition, the internal walls of the soundproof room were protected by soundproof cotton to reduce the noise reflection.

The AWA14423L type microphone (Hangzhou Aihua Instruments Co., Ltd., Hangzhou, China) was used to measure the radiation noise. The AWA6290M+ type two channel signal analyzer was used for the radiation noise signal acquisition and analysis, moreover, 1/3 Octave analysis method was adopted. Further details regarding the measurement characteristics of instruments used in the system are listed in Table 2.

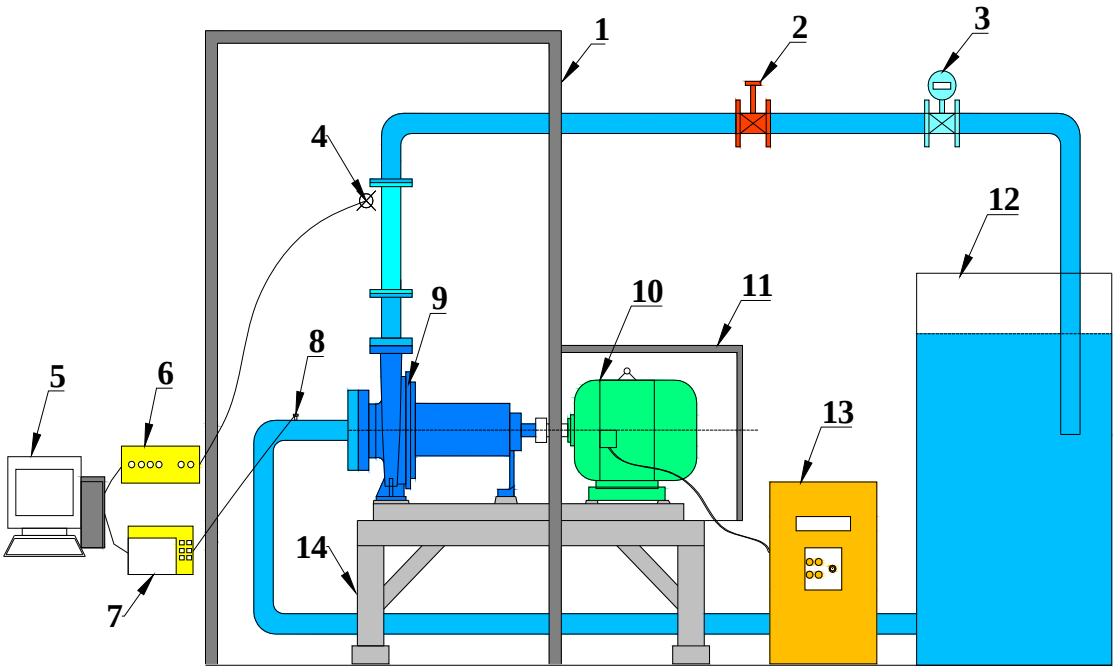

Figure 1. Layout and instrumentation of measurement system. 1: soundproof room; 2: valve; 3: flow meter; 4: radiation noise monitoring point; 5: computer; 6: two channel signal analyzer; 7: pressure recorder; 8: pressure monitoring point; 9: pump; 10: motor; 11: acoustic enclosure; 12: water tank; 13: frequency converter; and 14: bracket.

Table 2. Measurement characteristics of instruments.

Instruments	Type	Application	Measuring Range	Accuracy or Sensitivity
Flow meter	SLDG-800	Measuring flow rate	0–100 m^3/h	0.2% (accuracy)
Pressure transducer	MIK-300	Measuring inlet pressure	−100–0 kPa (inlet pipe)	0.5% (accuracy)
Pressure recorder	RX-200D	Recording pressure	/	/
Microphone	AWA14423L	Measuring radiation noise	10–20,000 Hz	50 mV/Pa (sensitivity)
Two channel signal analyzer	AWA6290M+	Analyzing radiation noise signal	/	/

Additionally, during the operation, the flow valve installed downstream on the outlet pipe was kept fully opened and unchanged. The pump was driven by the YVF2180L-2 type three-phase asynchronous motor and the rotational speed was regulated by the Y0300G3 type frequency converter, then the radiation noise frequency characteristics were studied under various rotational speeds. According to the similarity law, the relationship between rotational speed and flow rate is defined as,

$$\frac{Q_1}{Q_2} = \frac{n_1}{n_2} \tag{1}$$

where Q and n represent the flow rate and rotational speed, while the subscript 1 and 2 represent two different operation conditions. To ensure the safety of the running system, seven different rotational speeds that are less than or equal to rated rotational speed, i.e., varying from 1700 to 2900 rpm in increments of 200 rpm were considered. Table 3 shows the rotational speeds and corresponding flow rates.

Table 3. Rotational speeds and corresponding flow rates.

Rotational Speed, rpm	Flow Rate, m^3/h
1700	56.9
1900	64.8
2100	69.6
2300	74
2500	78.2
2700	82.1
2900	86

2.3. Arrangement of the Monitoring Points

To acquire the frequency distribution characteristics of radiation noise in different direction and corresponding amplitudes, 16 monitoring points were arranged on the measurement surface around the pump. As shown in Figure 2, the monitoring points were 1000 mm away from the center of the impeller and arranged evenly in a circumferential direction [26]. During the measurement process, the SPL of every monitoring point was measured sequentially by a microphone. Here, SPL is defined as,

$$SPL = 20log\frac{P_e}{P_{ref}} \tag{2}$$

$$P_e = \sqrt{\frac{1}{T}\int_0^T p'^2 dt} \tag{3}$$

where P_{ref}, P_e and p' represent the reference sound pressure (2×10^{-5} Pa in air), effective sound pressure and instantaneous sound pressure, respectively. Additionally, acoustic energy was introduced to compare the proportion of radiation noise in different frequency ranges because it can be superimposed by arithmetic, moreover, the propagation of sound is essentially the propagation of energy. Briefly,

the application of acoustic energy can reveal the proportion of radiation noise in different frequency ranges to overall noise intuitively. Therefore, the average acoustic energy density [27] is analyzed and it is defined as,

$$\varepsilon = \frac{P_e^2}{\rho c^2} \tag{4}$$

where ε, ρ and c represent the acoustic energy density, medium density (1.29 kg/m^3 in air) and the sound speed in medium (343 m/s in air), respectively.

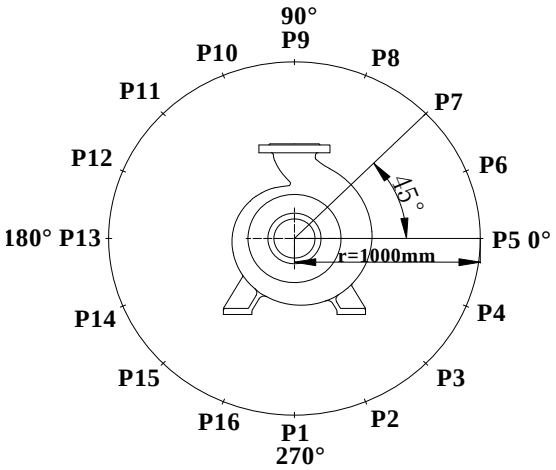

Figure 2. Arrangement of monitoring points in a circumferential direction.

To figure out the radiation noise overall intensity of the 16 monitoring points at certain frequencies, total sound pressure level (TSPL) is introduced and expressed as,

$$TPSL = 10lg\sum_{i=1}^{16} 10^{SPL_i/10} \tag{5}$$

3. Frequency Characteristics of Radiation Noise under Various Rotational Speeds

3.1. Changing Patterns of Radiation Noise in a Wide Frequency Range

By measuring the SPL characteristics of different monitoring points in a circumferential direction, the changing patterns of radiation noise in a wide frequency range were studied.

P1 (270°, in the direction against the outlet), P5 (0°, the minimum noise point), P9 (90°, in the direction facing the outlet) and P13 (180°, the minimum noise point) [28] are selected. Figure 3 illustrates the frequency characteristics of the four monitoring points in a wide range of frequencies. It can be observed that at rated rotational speed (2900 rpm), the SPLs of different monitoring points show a fluctuating ascending trend in the low frequency range from 31.5 to 1000 Hz, due to the excitation results of periodic interference between the impeller and volute [29], according to Equations (6) and (7),

$$f_{bpf} = \frac{nz}{60}1 \tag{6}$$

$$f_{spf} = \frac{n}{60}l \tag{7}$$

where f_{bpf} and f_{spf} represent BPF and shaft-passing frequency (SPF), z is the number of blades and l is harmonic sequence number (l = 1, 2, 3, . . .), SPLs reach a peak value at each order of BPF and SPF.

Unlike the frequency characteristics of flow noise in pump pipelines [11], the maximum value of radiation noise outside the pump appears in the range from 1000 to 2000 Hz, i.e., in the range of high order harmonics of BPF. The possible reason is that the native vibration frequencies of pump structure

belong to this range [30]. After that, the SPLs of different monitoring points decrease gradually when the frequency is higher than 2000 Hz. Besides, the SPLs at most frequencies of P9 are generally higher than those of other monitoring points. This can be explained by that P9 is located in an outlet direction, the radiation noise at P9 is more affected by the internal flow noise in the outlet pipeline and the vibration of the outlet pipeline.

In addition, the radiation noise frequency characteristics of P9 under various rotational speeds are compared in Figure 4. The radiation noise shows the same pattern of changes as those shown in Figure 3 under various rotational speeds. Moreover, with the increase in rotational speed, SPLs at various frequencies show an ascending trend and reach a maximum at 2900 rpm.

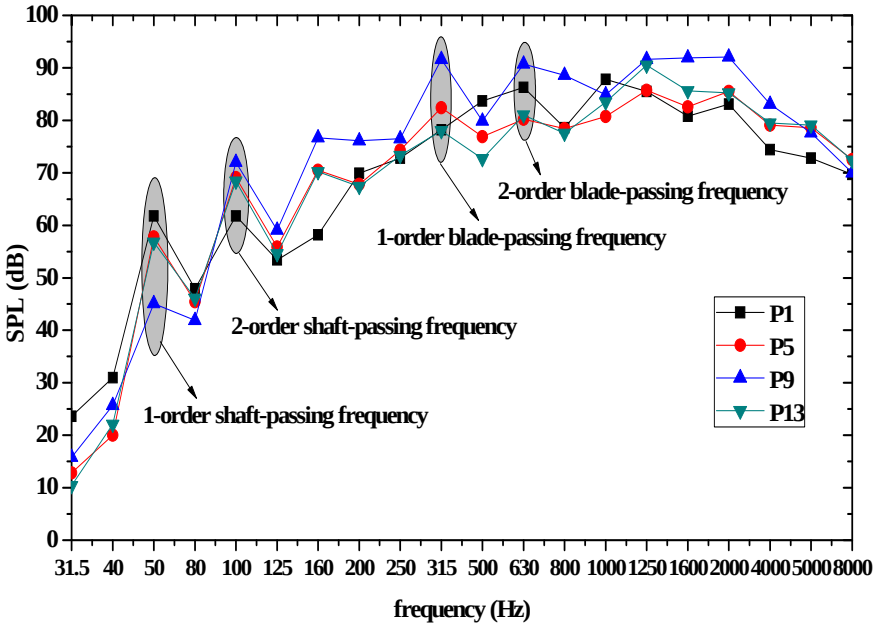

Figure 3. Changes in sound pressure level (SPL) at different monitoring points in a wide frequency range (2900 rpm).

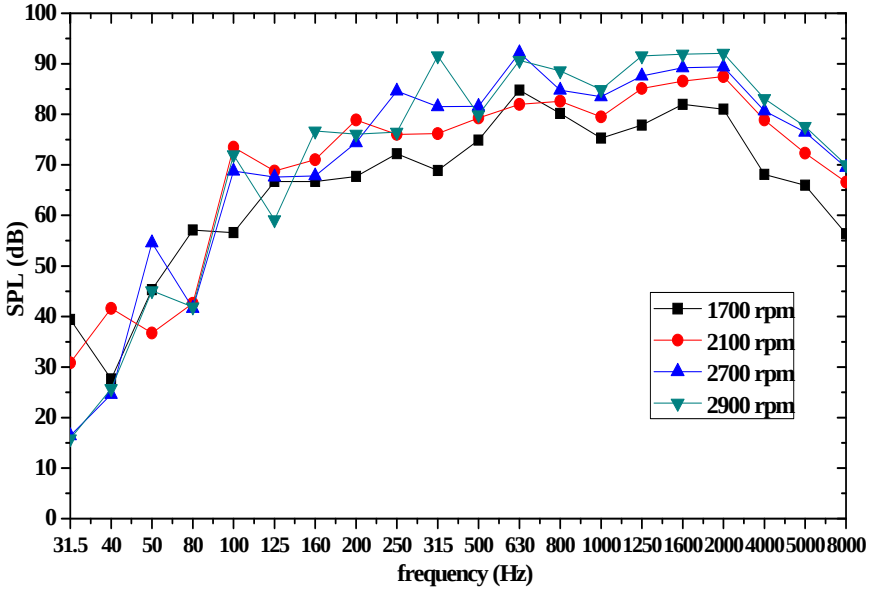

Figure 4. Changes in SPL in a wide frequency range under various rotational speeds (P9).

3.2. Changing Patterns of Radiation Noise in Different Frequency Ranges

As mentioned above, SPLs reach a maximum between 1000 and 2000 Hz. The noise in this range also belongs to the resonant frequency range of the ear cavity and has the greatest impact on people [31], so it is necessary to find out its proportion to overall noise. Therefore, the proportion of radiation noise in different frequency ranges to overall noise is studied quantitatively. The ratio of acoustic energy in the range from 0 to 1000 Hz (ε_1), 1000 to 2000 Hz (ε_2), as well as from 2000 to 8000 Hz (ε_3) to the total acoustic energy (ε_t) was analyzed under various rotational speeds.

Figure 5 shows the proportion of the acoustic energy in different frequency ranges to the total acoustic energy under various rotational speeds. In general, the radiation noise between 1000 and 2000 Hz makes the most significant contribution to overall noise, the value of $\varepsilon_2/\varepsilon_t$ is higher than 0.5 and increases by 22.61% when rotational speed increases from 1700 to 2900 rpm. Moreover, the acoustic energy between 0 and 1000 Hz accounts for about 0.30 of the total acoustic energy, however, the proportion decreases by 38.55% when rotational speed increases from 1700 to 2900 rpm. The change in rotational speed affects not only the radiation noise levels at different frequencies, but the proportion of radiation noise in different ranges, specifically, the increase in rotational speed causes an increase in the proportion of radiation noise from 1000 to 2000 Hz and a decrease in the proportion of radiation noise from 0 to 1000 Hz. When the frequency is higher than 2000 Hz, the radiation noise contributes very little to overall noise, but the proportion of this range shows little change with a change in rotational speed and the value of $\varepsilon_3/\varepsilon_t$ fluctuates around 0.12.

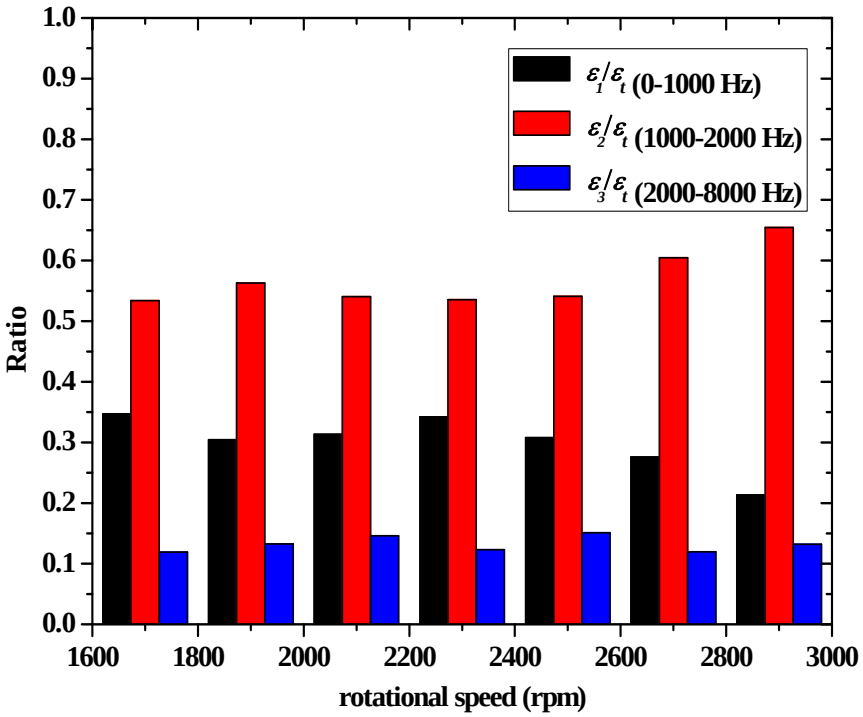

Figure 5. The ratio of acoustic energy in different frequency ranges.

3.3. Changes in Radiation Noise at Certain Frequencies

In this section, the changes in radiation noise at certain frequencies were studied. TSPLs of 16 monitoring points were calculated and the results of TSPLs at 500, 1000, 2000, 4000, 8000 Hz with various rotational speeds were compared and are presented in Figure 6.

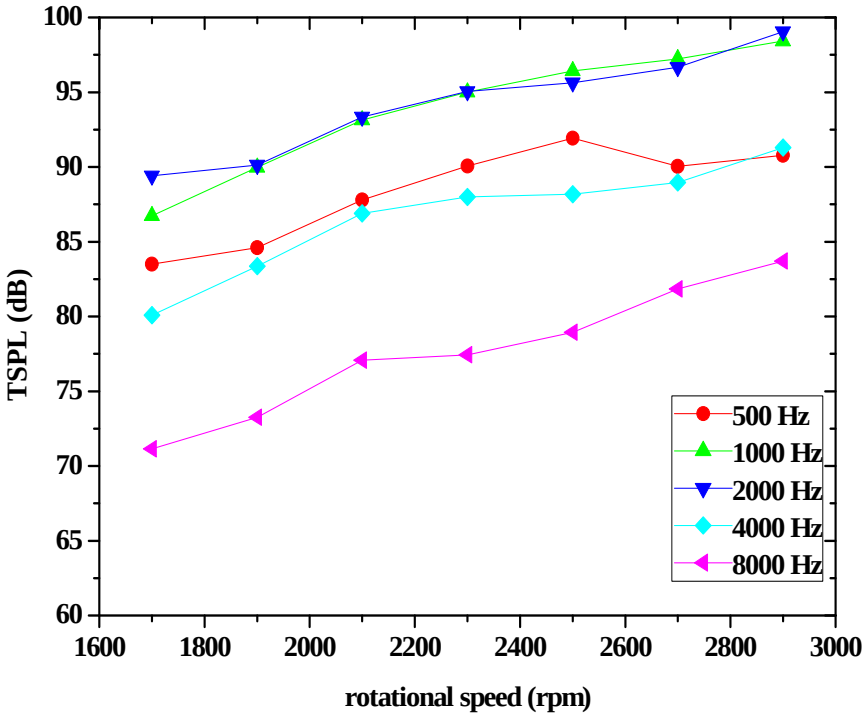

Figure 6. Changes in total sound pressure level (TSPL) at certain frequencies under various rotational speeds.

As shown in Figure 6, TSPLs at 1000 and 2000 Hz are higher than the others, while TSPL at 8000 Hz is lower than the others under all of the operational conditions. Additionally, there is a TSPL turning point at 500 Hz when rotational speed is set as 2500 rpm, which is the 2-order BPF under 2500 rpm. Moreover, TSPLs at various frequencies show an ascending trend with the increase in rotational speed and the increase in TSPL at high frequency is higher than at low frequency. More specifically, when rotational speed increases from 1700 to 2900 rpm, TSPLs at 500, 1000, 2000, 4000 and 8000 Hz increase 8.72%, 13.46%, 10.77%, 14.01% and 17.66%, respectively. On the one hand, with the increasing of rotational speed, the pressure fluctuation intensity on wall surfaces consequently increases [32], so TSPLs at various frequencies increase simultaneously. On the other hand, as the rotational speed increases, the required net positive suction head (NPSHr) also increases, however, the available net positive suction head (NPSHa) has different change rules, and is defined as,

$$NPSHa = \frac{p_s}{\rho g} + \frac{v_s^2}{2g} - \frac{p_v}{\rho g} \tag{8}$$

where p_s, v_s and p_v represent the inlet pressure (Pa), inlet velocity (m/s) and saturated vapor pressure at the corresponding temperature (25 °C). The NPSHa and NPSHr change patterns under various rotational speeds are presented in Figure 7.

As shown in Figure 7, with an increase in rotational speed, the NPSHa decreases immediately and is even lower than NPSHr under 2700 and 2900 rpm. The decrease in NPSHa can lead to the development of cavitation. Furthermore, the development of cavitation can cause both pump body vibration [33] and acoustic pressure pulsation [34], especially in high frequency ranges, and further cause a dramatic increase in radiation noise at high frequencies.

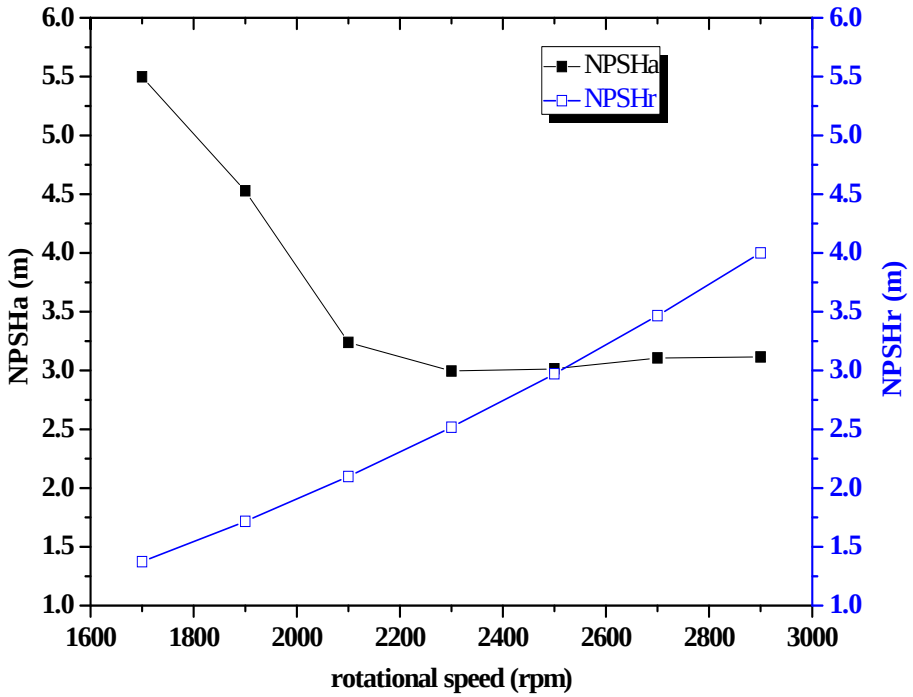

Figure 7. Changes in available net positive suction head (NPSHa) and required net positive suction head (NPSHr) under various rotational speeds.

4. Conclusions

In this study, a centrifugal pump radiation noise measurement system was established in a soundproof room, then the changing rules of radiation noise in a wide range of frequencies and the proportion of noise in different frequency ranges to overall noise, as well as the noise at certain frequencies were studied under various rotational speeds. The main conclusions are drawn as follows:

(1) Sound pressure levels (SPLs) at different monitoring points show a fluctuating ascending trend in the low frequency range from 31.5 to 1000 Hz, then reach a maximum value between 1000 and 2000 Hz and this is also the main contribution range to overall noise. When the frequency is higher than 2000 Hz, SPLs decrease gradually. Additionally, SPLs at most frequencies of the monitoring points in the outlet direction are generally higher than those of other monitoring points.

(2) The acoustic energy between 1000 and 2000 Hz accounts for more than half of the total acoustic energy and the proportion also increases by 22.61% when rotational speed increases from 1700 to 2900 rpm. While the acoustic energy between 0 and 1000 Hz accounts for about 0.30, the proportion in this range shows a decreasing trend and decreases by 38.55%. When frequency is higher than 2000 Hz, however, the radiation noise contributes very little to overall noise, the acoustic energy between 2000 and 8000 Hz accounts for about 0.12, but the proportion shows little change with the change of rotational speed.

(3) With increasing rotational speed, total sound pressure levels (TSPLs) at various frequencies increase gradually and the increase of radiation noise at high frequency is higher than that at low frequency, specifically, when rotational speed increases from 1700 to 2900 rpm, TSPLs at 500, 1000, 2000, 4000 and 8000 Hz increase 8.72%, 13.46%, 10.77%, 14.01% and 17.66%, respectively.

Author Contributions: C.G., D.L. designed the study, conducted the experiment and collected the experimental data; H.G. analyzed the experimental data; C.G. wrote the manuscript; M.G. reviewed and edited the manuscript.

Acknowledgments: This paper is supported by National Natural Science Foundation of China (No. 51776111) and Shandong Province Natural Science Foundation (No. ZR2016EEM35).

Conflicts of Interest: The authors declare no conflict of interest.

References

1. Tao, Z.; Yong'ou, Z.; Huajiang, O.; Tao, G. Flow-induced Noise and Vibration Analysis of a Piping Elbow with/without a Guide Vane. *J. Mar. Sci. Appl.* **2014**, *13*, 394–401.
2. Mattia, B.; Mario, I.; Raffaele, T.; Luigi, F. Combined CFD-Stochastic Analysis of an Active Fluidic Injection System for Jet Noise Reduction. *Appl. Sci.* **2017**, *7*, 623. [CrossRef]
3. Yong-Ju, C.; Yong-Sang, S.; Seung-Yop, L. Aerodynamic Analysis and Noise-Reducing Design of an Outside Rear View Mirror. *Appl. Sci.* **2018**, *8*, 519. [CrossRef]
4. Shah, S.R.; Jain, S.V.; Patel, R.N.; Lakhera, V.J. CFD for centrifugal pumps: A review of the state-of-the-art. *Procedia Eng.* **2013**, *51*, 715–720. [CrossRef]
5. Wu, D.F.; Liu, Y.S.; Li, D.L.; Zhao, X.F.; Li, C. Effect of materials on the noise of a water hydraulic pump used in submersible. *Ocean Eng.* **2017**, *131*, 107–113. [CrossRef]
6. Zhou, Y.L.; Yin, Y.X.; Zhang, Q.Z. Active control of repetitive impulsive noise in a non-minimum phase system using an optimal iterative learning control algorithm. *J. Sound Vib.* **2013**, *332*, 4089–4102. [CrossRef]
7. Brennen, C.E. A review of the dynamics of cavitating pumps. *J. Fluids Eng.* **2012**, *135*, 061301. [CrossRef]
8. Rzentkowski, G.; Zbroja, S. Experimental characterization of centrifugal pumps as an acoustic source at the blade-passing frequency. *J. Fluids Struct.* **2000**, *14*, 529–558. [CrossRef]
9. Rzentkowski, G.; Zbroja, S. Acoustic characterization of a CANDU primary heat transport pump at the blade-passing frequency. *Nucl. Eng. Des.* **2000**, *196*, 63–80. [CrossRef]
10. Parrondo, J.; Pérez, J.; Barrio, R.; González, J. A simple acoustic model to characterize the internal low frequency sound field in centrifugal pumps. *Appl. Acoust.* **2011**, *72*, 59–64. [CrossRef]
11. Si, Q.R.; Yuan, S.Q.; Yuan, J.P.; Yang, J. Flow-induced Noise Calculation of Centrifugal Pumps Based on CFD/CA Method. *J. Mech. Eng.* **2013**, *49*, 177–184. [CrossRef]
12. Yang, J.; Yuan, S.Q.; Yuan, J.P.; Si, Q.R.; Pei, J. Numerical and Experimental Study on Flow-induced Noise at Blade-passing Frequency in Centrifugal Pumps. *Chin. J. Mech. Eng.* **2014**, *27*, 606–614. [CrossRef]
13. Ke, B. Study on hydrodynamic noise of centrifugal pump in different operation conditions. *Technol. Acoust.* **2016**, *35*, 92–96.
14. Ye, X.M.; Pei, J.J.; Li, C.X.; Liu, Z. Experimental Study on Nosie Characteristics of Centrifugal Pump Based on Near-Field Acoustic Pressure Method. *Chin. J. Power Eng.* **2013**, *33*, 375–380.
15. Jeon, W.H.; Lee, D.J. A numerical study on the flow and sound fields of centrifugal impeller located near a wedge. *J. Sound Vib.* **2003**, *266*, 785–804. [CrossRef]
16. Jeon, W.H. A numerical study on the effects of design parameters on the performance and noise of a centrifugal fan. *J. Sound Vib.* **2003**, *265*, 221–230. [CrossRef]
17. Khelladi, S.; Kouidri, S.; Bakir, F.; Rey, R. Predicting tonal noise from a high rotational speed centrifugal fan. *J. Sound Vib.* **2008**, *313*, 113–133. [CrossRef]
18. Wang, M.; Freund, J.B.; Lele, S.K. Computational prediction of flow-generated sound. *Annu. Rev. Fluid Mech.* **2005**, *38*, 483–512. [CrossRef]
19. Sanghyeon, K.; Cheolung, C.; Warn-Gyu, P. Numerical Investigation into Effects of Viscous Flux Vectors on Hydrofoil Cavitation Flow and Its Radiated Flow Noise. *Appl. Sci.* **2018**, *8*, 289. [CrossRef]
20. Langthjem, M.A.; Olhoff, N. A numerical study of flow-induced noise in a two-dimensional centrifugal pump. Part I. Hydrodynamics. *J. Fluids Struct.* **2004**, *19*, 349–368. [CrossRef]
21. Langthjem, M.A.; Olhoff, N. A numerical study of flow-induced noise in a two-dimensional centrifugal pump. Part II. Hydroacoustics. *J. Fluids Struct.* **2004**, *19*, 369–386. [CrossRef]
22. Huang, J.X.; Geng, S.J.; Wu, R.; Liu, K.; Nie, C.Q.; Zhang, H.W. Comparison of noise characteristics in centrifugal pumps with different types of impellers. *Acta Acoust.* **2010**, *35*, 113–118.
23. Gao, M.; Dong, P.X.; Lei, S.H.; Turan, A. Computational Study of the Noise Radiation in a Centrifugal Pump When Flow Rate Changes. *Energies* **2017**, *10*, 221. [CrossRef]
24. Liu, H.L.; Dai, H.W.; Ding, J.; Tan, M.G.; Wang, Y.; Huang, H.Q. Numerical and experimental studies of hydraulic noise induced by surface dipole sources in a centrifugal pump. *J. Hydrodyn.* **2016**, *28*, 43–51. [CrossRef]
25. Ding, J.; Liu, H.L.; Wang, Y.; Tan, M.G.; Cui, J.B. Numerical study on the effect of blade outlet angle on centrifugal pump noise. *J. Vib. Shock* **2014**, *33*, 122–127.

26. Tao, J.Y.; Lu, X.N.; Wang, L.L. *Methods of Measuring and Evaluating Noise of Pumps*; Chinese Quality Supervision Bureau: Beijing, China, 2013.
27. Du, G.H.; Zhu, Z.M.; Gong, X.F. *Fundamentals of Acoustics*; Nanjing University Press: Nanjing, China, 2001.
28. Guo, C.; Gao, M.; Lu, D.Y.; Wang, K. An Experimental Study on the Radiation Noise Characteristics of a Centrifugal Pump with Various Working Conditions. *Energies* **2017**, *10*, 2139. [CrossRef]
29. Chu, S.; Dong, R.; Katz, J. Relationship between unsteady flow, pressure fluctuation, and noise in a centrifugal pump—Part B: Effects of blade-tongue interactions. *J. Fluids Eng.* **1995**, *117*, 30–35. [CrossRef]
30. Ma, Z.L.; Chen, E.Y.; Guo, Y.L.; Yang, A.L. Numerical Simulation of the Influence of the Diameter at the Outlet of an Impeller on the Noise Level Induced by the Flow Inside a Centrifugal Pump. *J. Eng. Therm. Energy Power* **2016**, *31*, 93–98.
31. Lu, D.Y. Experimental Study on Flow-Noise of Centrifugal Pump in Variable Working Condition. Master's Thesis, Shandong University, Jinan, China, 2017.
32. Dong, P.X.; Gao, M.; Guan, H.J.; Lu, D.Y.; Song, K.Q.; Sun, F.Z. Numerical simulation for variation law of volute radiated noise in centrifugal pumps under variable rotating speed. *J. Vib. Shock* **2017**, *36*, 128–133.
33. Wang, Y. Research on Cavitation and Its Induced Vibration and Noise in Centrifugal Pumps. Ph.D. Thesis, Jiangsu University, Zhenjiang, China, 2011.
34. Lu, J.X.; Yuan, S.Q.; Yuan, J.P.; Ren, X.D.; Pei, J.; Si, Q.R. Research on the noise induced by cavitation under the asymmetric cavitation condition in a centrifugal pump. In Proceedings of the 9th International Symposium on Cavitation, Lausanne, Switzerland, 6–10 December 2015.